Chapter 1

Introduction

1.1 A Star is Born

> *"Stars are the fundamental objects of astronomy; thus, the formation of stars constitutes one of the basic problems of astrophysics."*

So began the seminal paper on the theory of isolated low mass star formation by Shu, Adams, & Lizano (1987). Understanding how stars form has consequences not only for the current generation of star birth in our own Galaxy, but also for the existence of planets suitable for life, the evolution of galaxies, and the creation of the first heavy elements.

Our current general picture of how an isolated low mass star is born was driven largely by the work of Shu et al. (1987), which provided one of the first coherent paradigms detailing the formation of a star, beginning with the dense parent core and continuing until the young stellar object becomes optically visible as it evolves onto the main sequence. Despite significant progress over the last few decades, however, the formation of stars in our Galaxy remains one of the basic problems of astrophysics. The lack of a more complete understanding, especially regarding the earliest phases from the formation of dense cores through the end of the main accretion phase, is due in large part to the difficulty of observing stellar systems in their prenatal and infant phases, and to the complexity of the environments in which they form.

The basic framework on which we hope to build a more complete picture is summarized below in §1.1.1. It may be thought of as the pencil sketch of an unfinished

painting; important structural features are in place, but the details, subtleties, and true coherence of the image have yet to be completed. In fact, this general outline by no means represents a complete picture of low mass star formation; the majority of stars do not form in isolation, but in groups and clusters in molecular clouds. The formation of stars must be understood in the context of their birth sites, and to be complete our picture must include the formation of prestellar cores from the cloud medium. In §1.1.2 I outline a few of the most outstanding questions regarding the formation of low mass stars in molecular clouds. In the remainder of this chapter I discuss approaches for attacking those questions, and summarize the goals and outline of this thesis.

1.1.1 Working Model for Isolated Star Formation

What has become the standard schematic picture of how an isolated low mass star forms (Shu, Adams, & Lizano, 1987; Lada, 1987; André, Ward-Thompson, & Barsony, 1993), is shown in figure 1.1. Characteristic spectral energy distributions (SED) of the observationally defined classifications for Class 0 (André et al., 1993), Class I, II, and III (Lada & Wilking, 1984), are plotted on the left as $\log(\lambda F_\lambda)$ versus λ. In the center column are schematic depictions of what those SEDs may correspond to physically. Note that a direct association between Class 0 through Class II and a true evolutionary sequence remains a subject of debate (e.g. Jayawardhana, Hartmann, & Calvet, 2001), and timescales listed to the far right are highly uncertain, especially for the earliest phases (e.g. Visser, Richer, & Chandler, 2002).

Classes I–III were originally defined empirically by Lada & Wilking (1984) based on the SED shapes of infrared sources in the Ophiuchus molecular cloud. More specifically, objects were grouped into classes based on their near-infrared to mid-infrared spectral index. These morphological classifications were soon interpreted in terms of a physical evolutionary sequence (Adams, Lada, & Shu, 1987), based on the theoretical models of Adams & Shu (1986). Class I sources are associated in this evolutionary sequence with protostars during their main infall stage, surrounded by

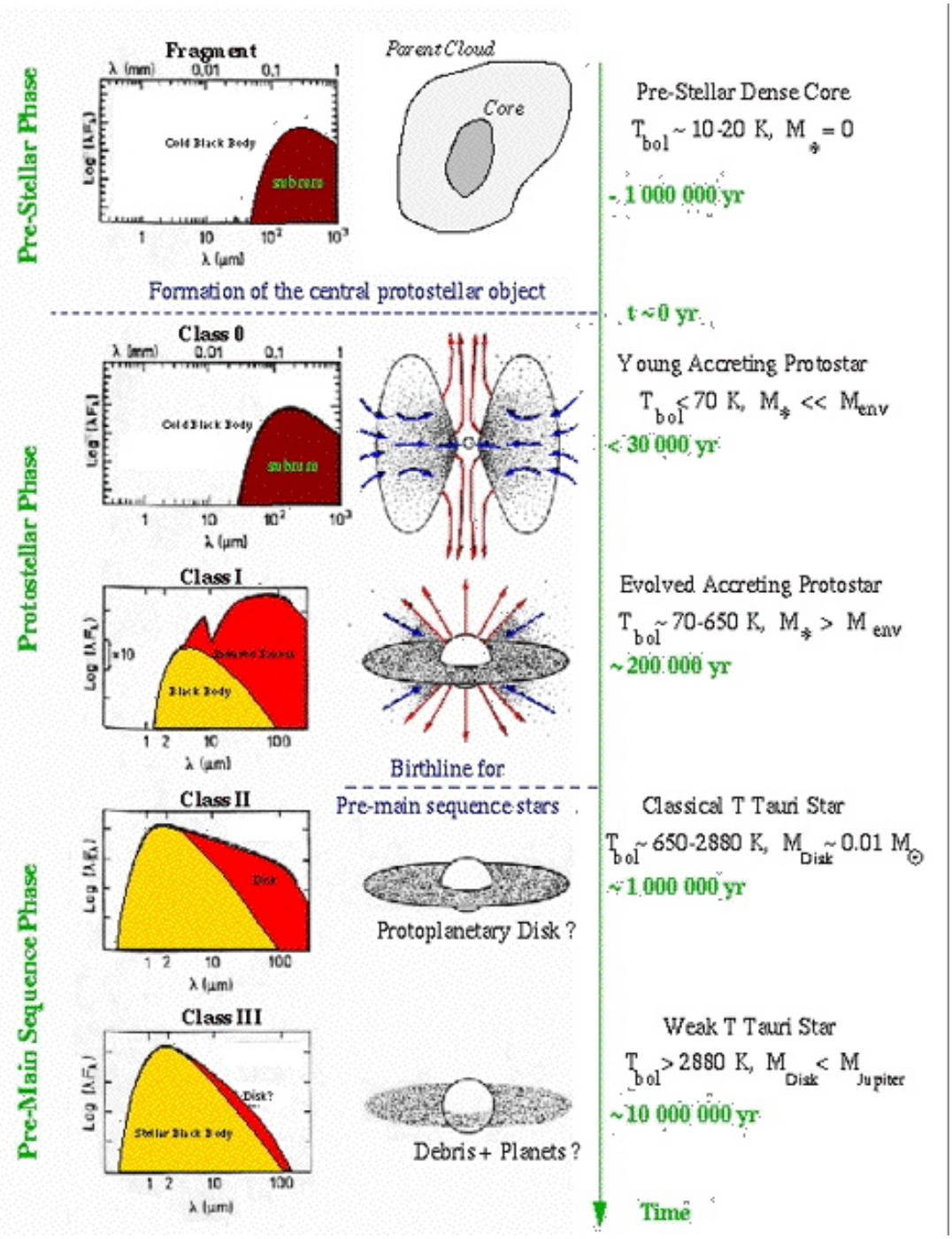

Figure 1.1 Standard schematic picture of how an isolated low mass star forms, originally adapted from André (1994), Shu et al. (1987), and Wilking (1989). Observationally classified SEDs are shown on the left, with the proposed physical interpretations (Adams et al., 1987; André et al., 1993) in the center column. Evolution proceeds from top to bottom, but the associated timescales are highly uncertain.

a rotating disk and infalling dusty envelope (Adams et al., 1987). More recently, Class I sources have been associated with an evolutionary state in which the mass of the accreting protostar exceeds the mass of the infalling envelope: $M_* > M_{env}$ (André & Montmerle, 1994). The Class I SED shown in figure 1.1 arises primarily as a result of reprocessed emission from the disk and envelope.

Accretion from the envelope onto the protostar occurs through a rotating accretion disk (e.g., Shu et al., 1993). The dissipation of kinetic energy of infalling material in an accretion shock at the hydrostatic surface of the protostar provides the primary source of luminosity:

$$L_{acc} \sim \frac{GM_*\dot{M}}{R_*}, \tag{1.1}$$

where M_*, R_* are the mass and radius of the central protostar, and $\dot{M} = dM/dt$ is the mass accretion rate (Shu et al., 1987). Class I sources are observed to have well-collimated bipolar outflows, which create a cavity in the envelope and interact with the surrounding cloud medium to produce large-scale molecular outflows (Bachiller, 1996).

When infall is terminated by a widening stellar wind or outflow, the object becomes optically visible and enters Class II, with a passive nebular disk reprocessing emission from the pre-main sequence star (Adams et al., 1987). Class II or classical T Tauri stars are characterized by an SED that peaks in the near-infrared and resembles a stellar photosphere with excess emission from a remnant disk at longer wavelengths. After removal of the nebular disk, the SED of the Class III or weak T Tauri star is that of a reddened photosphere (Lada, 1987).

Later, observations of submillimeter condensations (cores) revealed a population of such cores that were invisible in the near-infrared but showed indirect evidence for a central protostar, such as a compact radio continuum source, collimated bipolar outflow, or a source of internal heating (e.g., André, 1996). Thus the Class 0 phase was added to the classification scheme to accommodate sources with SEDs peaking at long wavelengths but evidence of a protostellar nature (André et al., 1993). André & Montmerle (1994) interpreted Class 0 sources as a younger stage than Class I, when

the mass of the central protostar is still less than that of the surrounding envelope ($M_* < M_{env}$), although the validity of this interpretation has not been verified. The Class 0 SED is shown in figure 1.1 as a cold blackbody peaking at $\lambda \sim 100 - 200\mu$m, with all emission from the hot protostar absorbed by the dense envelope and re-emitted at long wavelengths. Recent *Spitzer* Space Telescope observations have shown that some Class 0 sources are detectable at $3.6 - 8\mu$m, however (e.g., Jørgensen et al., 2006).

Submillimeter cores similar to Class 0 sources but with no evidence for a central protostar likely represent the earliest prestellar phase, prior to core collapse and protostellar formation (Ward-Thompson et al., 1994). Shown at the top of figure 1.1, dense prestellar cores have no internal source of luminosity; they are heated from the outside by the interstellar radiation field, and the SED resembles that of a cold blackbody, peaking in the far-infrared (e.g., Myers & Benson, 1983). The lifetime of this prestellar phase depends strongly on the core formation process and the dominant physics in the cloud (e.g., Ward-Thompson et al., 2007).

The more evolved Class II and III sources, or pre-main sequence stars, are fairly well understood, as they do not have an obscuring envelope and thus are directly observable. In this thesis I will focus on the earlier stages, from prestellar cores to Class I, where I sometimes refer to Class 0/I as the "main accretion phase."

1.1.2 Outstanding Questions

In spite of the general framework described above, there remain a number of outstanding questions regarding the formation and early evolution of low mass stars. In reality, the star formation process begins on scales much larger than an individual core. The majority of stars are born in molecular clouds (e.g., Lada & Lada, 2003, and references therein), and their formation is governed by global physics such as turbulence and magnetic fields (e.g., Evans, 1999), as well as local processes such as outflows and rotation (e.g., Shu et al., 1987). The relative importance of these processes are still not well understood. Details of the early evolution of protostel-

lar sources are extremely uncertain, including mass accretion rates during the Class 0 and Class I phases. In addition, measurements of the timescales associated with the earliest stages vary considerably, ranging from 10^5 to 10^7 yr for prestellar cores (Ward-Thompson et al., 2007) and from 10^4 to a few $\times 10^5$ yr for Class 0 (André & Montmerle, 1994; Visser et al., 2002). In fact, the association of Class 0 and Class I with distinct evolutionary stages is still a matter of debate (e.g., Jayawardhana et al., 2001).

The primary questions that will be investigated in this thesis are:

(1) What are the global physical processes controlling the formation and support of prestellar cores and their subsequent collapse into protostars?
(2) What are the initial conditions of star formation, as traced by the prestellar core populations of molecular clouds?
(3) After core collapse, how do protostars evolve through the earliest phases, including mass accretion rates and timescales?
(4) How does the star formation process depend on environmental factors such as average cloud density or the strength of turbulence?

1.1.3 Global Processes: Magnetic Fields versus Turbulence

The mass and spatial distributions of prestellar cores retain imprints of their formation process, and the lifetime of those cores is extremely sensitive to the dominant physics controlling their formation. Understanding the properties of prestellar cores on cloud scales, and how they vary with environment, provides insight into the global physical processes controlling star formation in molecular clouds.

It has long been accepted that Galactic molecular clouds cannot be in free-fall collapse (Zuckerman & Palmer, 1974). Given the typical masses of clouds ($M > 10^4$ $M_\odot$), together with the Jeans mass for average cloud conditions ($M_J \lesssim 80$ $M_\odot$), this conclusion implies that some additional means of support beyond thermal pressure is required (see Evans 1999 for a review). Magnetic fields and large-scale turbulence are the most likely candidates for this additional support, and both provide mechanisms

for the formation of self-gravitating cores, and subsequent collapse (Shu et al., 1987; Mac Low & Klessen, 2004). In a general sense, magnetic fields are associated with the slow, quasi-static evolution of prestellar cores, while turbulence is associated with a more rapid, dynamic evolution.

In the Shu et al. (1987) paradigm (hereafter the Shu model), magnetic fields dominate the support of molecular clouds on large scales, and low mass star formation takes place in magnetically sub-critical clouds. The relevant parameter is the ratio of magnetic field energy density to gravitational potential energy: E_B/E_G. For $E_B/E_G = 1$ the region will be magnetically critical, while $E_B/E_G < 1$ and $E_B/E_G > 1$ indicate sub-critical and super-critical regions, respectively. In the highly sub-critical case, ambipolar diffusion moderates the quasi-static contraction of prestellar cores with masses exceeding the local Jeans mass (Shu et al., 1987):

$$M_J = \frac{a^3}{\rho^{1/2} G^{3/2}}, \tag{1.2}$$

where a is the thermal sound speed and ρ is the mass density (Jeans, 1928).

Neutral particles are supported against self-gravity only by their friction with ionized particles, which are tied to the magnetic field; ambipolar diffusion refers to the process by which neutrals slip relative to the ions (Spitzer, 1968). The relevant timescale is the ambipolar diffusion timescale:

$$t_{AD} = \frac{3}{4\pi G \rho \tau_{n_i}} \simeq 7.3 \times 10^{13} x_e \text{ yr}, \tag{1.3}$$

where τ_{n_i} is the ion-neutral collision time and x_e is the ionization fraction (e.g., Evans, 1999). For typical cloud conditions, $t_{AD} \sim 10 t_{ff}$ (Nakano, 1998), where t_{ff} is the free-fall timescale (Spitzer, 1978):

$$t_{ff} = \sqrt{\frac{3\pi}{32 G \rho}}. \tag{1.4}$$

Although slow, quasi-static evolution of prestellar cores toward collapse is typically associated with magnetic field support, the gradual dissipation of low level turbulence

can also lead to quasi-static evolution (Myers, 1998).

Molecular clouds are known to be turbulent, with supersonic line widths (e.g., McKee & Zweibel, 1992), and the idea that turbulence dominates the star formation process has gained prevalence in recent years. This is due in part to a number of observations that seem to be inconsistent with the standard Shu model, including the measured density profiles of cores, and the inferred lifetimes of various protostellar phases (see Mac Low & Klessen 2004 for a review). Furthermore, simulations of turbulent fragmentation have had some success reproducing the shape of the initial mass function of stars (e.g., Padoan & Nordlund, 2002; Li et al., 2004). If highly turbulent processes dominate molecular cloud evolution, then detailed models suggest that the lifetime of prestellar cores should be short, approximately $1 - 2\ t_{ff}$ (Ballesteros-Paredes, Klessen, & Vázquez-Semadeni, 2003; Vázquez-Semadeni et al., 2005). Even if magnetic fields are present, cores will collapse on approximately the free-fall timescale as long as the region is super-critical.

Thus, the lifetime of prestellar cores should be a strong discriminator of core formation mechanisms. Published measurements of the prestellar core lifetime vary by two orders of magnitude, however. For example, based on the fraction of optically selected cores with mean densities of $6 - 8 \times 10^3$ cm^{-3} observed by Lee & Myers (1999) to be starless, a core lifetime of 6×10^5 yr was suggested. This is a factor of ~ 20 shorter than the ambipolar diffusion timescale. The fraction of starless isolated globules detected in NH_3 by Bourke et al. (1995) implies a lifetime of 2×10^6 yr. By contrast, Jessop & Ward-Thompson (2000) find a lifetime of 10^7 yr, similar to the ambipolar diffusion timescale, for low density cores detected from column density maps based on IRAS far-infrared observations. Most recently, using SCUBA and *Spitzer* maps of Perseus, Jørgensen et al. (2007); Hatchell et al. (2007) both find starless core lifetimes of a few $\times 10^5$ yr.

The implications of these results can be seen in figure 1.2, from Ward-Thompson et al. (2007), which compares the inferred starless core lifetime from earlier published studies with the mean volume density for each sample. In this figure, the lower dashed line represents the free-fall timescale t_{ff} as a function of mean density, and the upper

line indicates $10\,t_{ff}$, approximately the ambipolar diffusion timescale. Most points fall between these two extremes, suggesting that (a) starless cores have some additional means of support beyond thermal pressure, and (b) that cores are unlikely to be highly magnetically sub-critical. Uncertainties in the contributing measurements are large, however, and the number of studies for cores with mean densities greater than approximately $10^4 - 10^5$ cm^{-3} are relatively few. Cores with densities less than 10^4 cm^{-3} may not be truly prestellar, so lifetime arguments based on such objects may be biased.

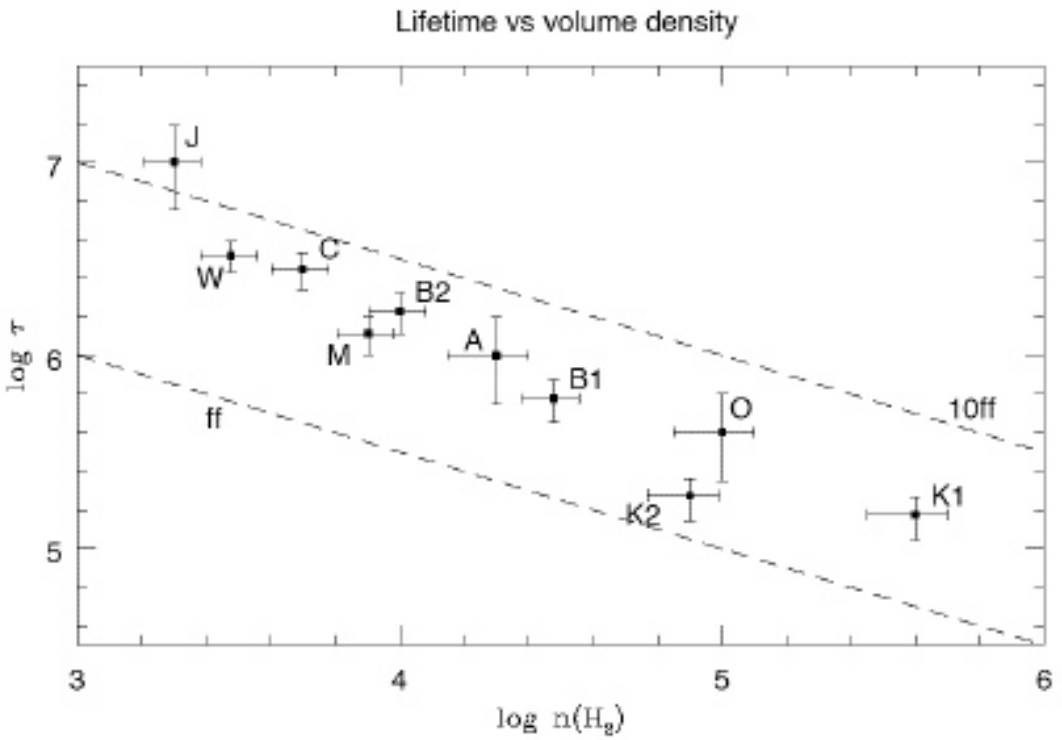

Figure 1.2 Correlation between measured starless core lifetime and the mean density of the sample for a number of studies published before 2006, from Ward-Thompson et al. (2007). Dashed lines indicate the free fall timescale (lower), and $10t_{ff}$, or approximately the ambipolar diffusion timescale (upper). The distribution of measurements suggests that cores have some non-thermal support, but are not highly sub-critical.

Another possible discriminator of global cloud physics is the existence of a column density, or A_V, threshold for star formation. Scenarios in which magnetic fields are the dominant force in molecular clouds naturally accommodate such a threshold, since the support of cloud material by magnetic fields requires the presence of ionized

particles. Core collapse cannot occur if the ionization fraction is too high, but in cloud interiors where material is shielded from cosmic rays, the lower ionization fractions allow for the formation and collapse of cores via ambipolar diffusion. McKee (1989) estimates that star formation requires a minimum column density of $A_V \sim 4-8$ mag, while Shu et al. (1987) suggest $A_V > 4(B/30\mu G)$ mag. While a few authors claim to have observed such an A_V threshold (Palla & Stahler, 2002; Johnstone, DiFrancesco, & Kirk, 2004), the supporting evidence is hardly robust, and further observations are required. As noted by Johnstone et al. (2004), it is not clear how turbulent models of star formation could produce an A_V threshold, so confirmation of such a threshold would provide support for the importance of magnetic fields in the star formation process.

1.1.4 Core Initial Conditions

The initial conditions of dense star-forming cores depend strongly on the physical processes leading to their formation (§1.1.3). In turn, core properties help to determine the evolution of newly formed protostars, as will be demonstrated in §1.1.5. One of the most important diagnostics of initial conditions is the mass distribution of prestellar cores. In addition to being a testable prediction of core formation models, a comparison of the core mass distribution (CMD) to the stellar initial mass function (IMF) may reveal what process is responsible for determining stellar masses (e.g., Meyer et al., 2000).

We focus on three possible processes in the determination of a star's final mass, the value of which fixes its subsequent evolution: (1) In the Shu paradigm, a star determines its own destiny. Cores evolve toward a singular isothermal sphere (SIS) configuration before collapse, and the accreting protostar has, by definition, an infinite mass supply. Accretion is self-regulating, halted by a stellar wind or outflow that is triggered by the onset of thermonuclear burning and clears out the remaining envelope material. The final mass of the star depends primarily on the accretion rate (Shu,

1977):

$$\dot{M} = m_0 a^3/G, \tag{1.5}$$

and thus on the sound speed in the initial core, since a is the effective sound speed and m_0 is a constant of order unity. (2) In the competitive accretion picture (e.g., Bonnell et al., 2001), the mass accretion of sources in clusters is a dynamic process. Sources that form earlier or are closest to the cluster center, where the gas density is higher, will have the highest accretion rates and thus the largest final masses. A strong similarity between the prestellar CMD and the final stellar IMF is not necessarily expected for either competitive accretion or the self-regulating Shu model. (3) Alternatively, the final mass of a star may be established during core formation, presumably by the fragmentation process. In crowded regions where the mass reservoir of any given protostar is limited to the core in which it formed, the final stellar mass will depend on the initial core mass. If this fraction is relatively universal, then the shape of the emergent IMF should mirror that of the CMD. The idea that cloud fragmentation leads directly to the IMF is by no means new, but the original idea of the formation of cores by hierarchical fragmentation (Hoyle, 1953) has largely been replaced by turbulent fragmentation (e.g., Mac Low & Klessen, 2004; Ballesteros-Paredes et al., 2006).

Of course, all three of these processes probably play some role. Given the current observational capabilities, we can realistically hope to test the hypothesis that the stellar IMF is entirely determined by the core fragmentation process, based on a comparison of the prestellar CMD to the IMF. While a direct link between the two cannot be definitively determined by comparing the mass distribution shapes, it is possible to either rule out or build evidence for such a link. Most often, the shape of both the IMF and CMD are approximated either by a power law:

$$\frac{dN}{dM} \propto M^{\alpha}, \tag{1.6}$$

where dN/dM is the differential mass distribution and α is the power law slope, or

by a lognormal function:

$$\frac{dN}{d\log M} = A \exp\left[\frac{-(\log M - \log M_0)^2}{2\sigma^2}\right], \tag{1.7}$$

where

$$\frac{dN}{dM} = \frac{1}{(\ln 10)M}\frac{dN}{d\log M}, \tag{1.8}$$

M_0 is the characteristic mass, and σ is the width of the distribution.

There is some evidence that the stellar IMF is universal within our Galaxy (e.g., Kroupa, 2002), but individual measurements of the IMF shape can vary significantly, and uncertainties remain large (e.g., Scalo, 2005). The classic value for the IMF slope is the "Salpeter IMF": $\alpha = -2.35$ (Salpeter, 1955), while Scalo (1986) found a steeper slope ($\alpha \sim -2.7$) for sources with mass $M \gtrsim 1$ $M_\odot$. More recently, Reid, Gizis, & Hawley (2002) find $\alpha \sim -2.5$ above 0.6 $M_\odot$, and $\alpha \sim -2.8$ above 1 $M_\odot$, while Schröder & Pagel (2003) find $\alpha \sim -2.7$ for $1.1 < M < 1.6$ $M_\odot$ and $\alpha \sim -3.1$ for $1.6 < M < 4$ $M_\odot$. Thus an IMF slope within the range $\alpha = -2.3$ to -2.8 appears to be a reasonable choice for $M > 1$ $M_\odot$.

Much recent work has focused on lower masses, where the IMF becomes flatter than the Salpeter or Scalo values, and may be better characterized by a lognormal function. Kroupa (2002) suggests a three-component power law: $\alpha = -2.3$ for $0.5 < M < 1$ $M_\odot$, $\alpha = -1.3$ for $0.08 < M < 0.5$ $M_\odot$, and $\alpha = -0.3$ for $0.01 < M < 0.08$ $M_\odot$, while Chabrier (2005) finds that a lognormal distribution with $\sigma = 0.55$ and $M_0 = 0.25$ $M_\odot$ is a good fit for $M < 1$ $M_\odot$. The system IMF, for which multiple systems are not resolved, is appropriate for comparison to core studies and peaks at approximately $0.2 - 0.3$ $M_\odot$ (e.g., Chabrier, 2005; Luhman et al., 2003). To date, a few studies have found similarities between the shapes of the IMF and CMD, providing support for the idea that stellar masses in clusters are determined by the fragmentation of turbulent clouds. Testi & Sargent (1998) measured the mass distribution of millimeter cores in the Serpens main core with the OVRO interferometer, finding a power law slope of $\alpha = -2.1$ above 0.4 $M_\odot$, similar to the Salpeter IMF. Similarly, Motte et al. (1998) found $\alpha = -2.5$ for submillimeter cores with $M > 0.5$ $M_\odot$ in the ρ Ophiuchi main

cloud, while Onishi et al. (2002) measured a slope for the mass distribution of starless $H^{13}CO^+$ $J = 1 - 0$ condensations in Taurus of $\alpha = -2.5$ for $M > 3.5$ $M_\odot$.

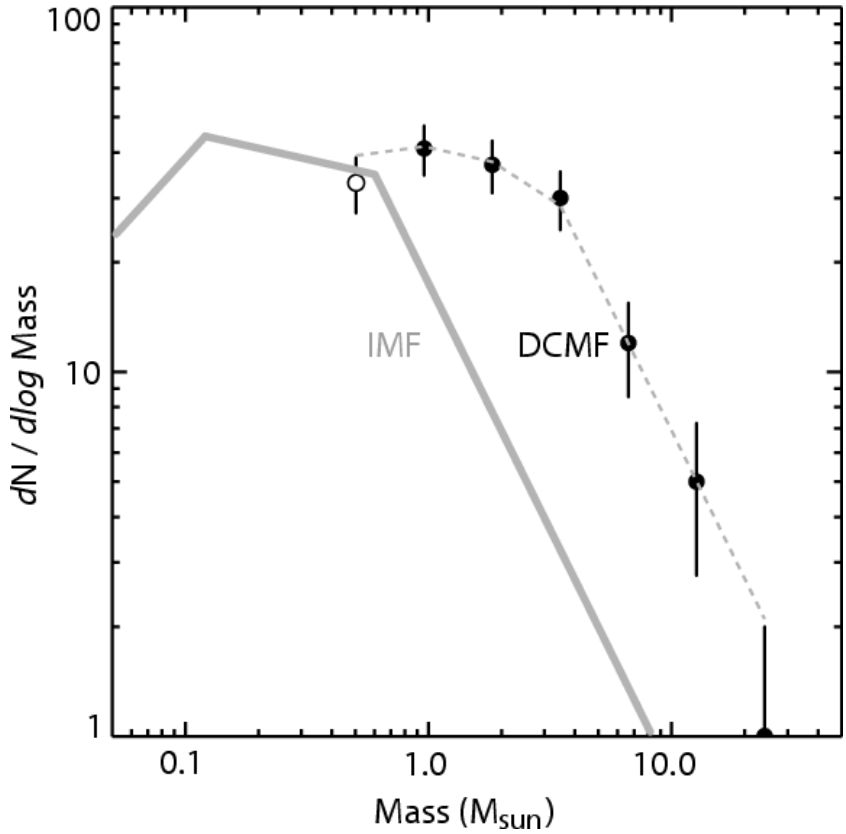

Figure 1.3 Mass distribution of cores in the Pipe nebula identified by dust extinction, from Alves et al. (2007). The shape of the CMD is remarkably similar to the shape of the stellar IMF measured by Muench et al. (2002) for the Trapezium cluster, with the CMD shifted to higher masses by approximately a factor of four.

More recently, Alves, Lombardi, & Lada (2007) used dust extinction toward the Pipe nebula to derive a CMD that is characterized by a two-component power law above 1 $M_\odot$, with a break at about 2.5 $M_\odot$(figure 1.3). The Pipe Nebula CMD appears remarkably similar to the stellar IMF for the Trapezium cluster (Muench et al., 2002), with the CMD shifted to higher masses by approximately a factor of four. Alves et al. (2007) interpret this similarity as evidence that the stellar IMF is a direct product of the CMD, with a uniform core-to-star efficiency of $30\% \pm 10\%$. The mean densities of the extinction-identified cores in this study ($5 \times 10^3 - 2 \times 10^4$ cm^{-3}) are lower than those of typical cores traced by dust (sub)mm emission ($\gtrsim 10^4$ cm^{-3}; chap-

ter 5), however, and the cores may not be truly prestellar. Furthermore, extinction measurements are sensitive to all material along the line of sight, and may confuse dense cores with more extended structures.

Large samples of prestellar cores are important for further addressing this problem, as is a more reliable separation of prestellar, protostellar, and unbound starless cores. Molecular line or extinction surveys often trace relatively low density material ($10^3 - 10^4$ cm^{-3}), leaving the possibility that such cores may never collapse to form stars. In addition, most previous studies base the identification of protostellar versus starless cores on near-infrared data, which is not sensitive to the most embedded protostars, or on low resolution and poor sensitivity IRAS maps. The first issue can be remedied by using millimeter or submillimeter surveys; (sub)mm emission traces dense ($n > 10^4$) material, and detection at (sub)mm wavelengths tends to correlate well with other indications of a true prestellar nature, such as in-falling motions (Gregersen & Evans, 2000). *Spitzer* provides significant progress on the second, with substantially superior resolution and sensitivity compared to IRAS, making the identification of prestellar cores much more secure.

Another revealing measure of core initial conditions is the radial density profile of prestellar cores. In the Shu model, cores forming via ambipolar diffusion evolve toward the radial density profile of a singular isothermal sphere, characterized by $\rho(r) \propto r^{-2}$, just before collapse. There are many possible initial configurations, however. Isothermal cores confined by external pressure, or Bonnor-Ebert spheres (Bonnor, 1956; Ebert, 1955), have a maximum density contrast from the center to the outer edge of 14, and an inner density profile that is significantly shallower than the SIS. The logotropic equation of state considered by McLaughlin & Pudritz (1997) corresponds to initial cores cores with $\rho(r) \propto r^{-1}$.

Two complementary methods may be employed to understand the density profiles of prestellar cores: high resolution studies of individual cores, or statistical arguments based on large samples. A number of recent studies using high resolution observations at (sub)mm wavelengths and radiative transfer modeling have found evidence for flattened inner density profiles, similar to BE spheres (Di Francesco et al., 2007). It

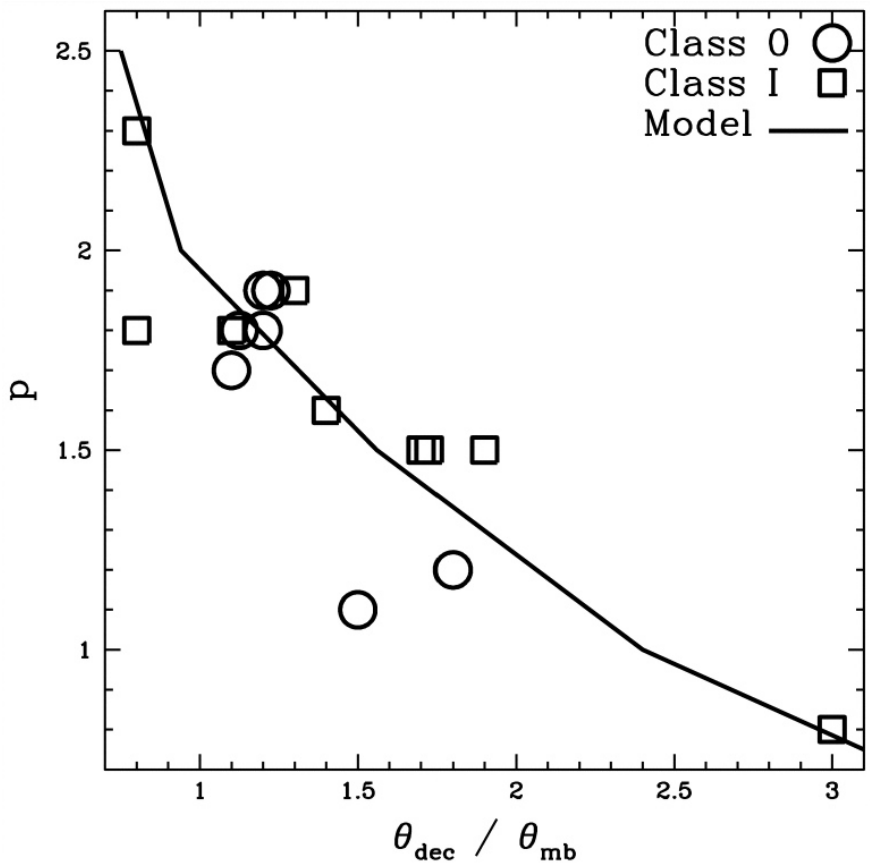

Figure 1.4 Correlation between source angular size and density profile, from Young et al. (2003). The density power law index p, inferred from radiative transfer modeling of Class 0 and Class I sources, is shown versus the measured angular deconvolved size, together with the relation predicted by dust emission models (solid line). This correlation provides a method for probing source density profiles with only marginally resolved data.

may also be possible to probe the density profile of starless cores with only marginally resolved data, if a sufficient sample size is assembled. Young et al. (2003) have shown that the measured angular deconvolved sizes θ_{dec} of sources with power law density profiles are inversely proportional to the index of the power law p. This is demonstrated in figure 1.4, from Young et al. (2003), where θ_{mb} is the beam full-width at half-maximum, and the observed p values for Class 0 and Class I sources were determined from radiative transfer modeling of SCUBA data. The solid line represents dust emission models with $0.5 < p < 2.5$. Using the correlation between p and θ_{dec} shown in figure 1.4, it is feasible to infer the average density power law index

of a large sample of sources based on their observed sizes. Although this analysis requires the assumption of a power law density profile, it is nonetheless possible to test the Shu model prediction that $p = 2$ for prestellar cores close to collapse.

1.1.5 Early Protostellar Evolution

Protostellar evolution is directly tied to initial conditions of cores, and accretion rates during the main accretion phase are an important discriminator for star formation models. The Shu model predicts a constant accretion rate, $\dot{M} \sim a^3/G$, while isothermal non-singular core density profiles generally result in rates that are initially high and decrease with time (e.g., Henriksen, Andre, & Bontemps, 1997). The logotropic core equation of state adopted by McLaughlin & Pudritz (1997), in contrast, produces accretion rates that increase with time as $\dot{M} \propto t^3$.

Directly measuring the accretion rates of newly formed protostars is nearly impossible due to their embedded nature (although $\dot{M}$ has been measured for a few optically visible Class I sources (White et al., 2007)). We can constrain these rates, however, using evolutionary models, which have been developed to reproduce the observed spectrum of protostellar sources as a function of time by varying initial conditions, mass accretion rates, and final stellar mass. Some models apply analytic solutions to the problem of core collapse (e.g., Myers et al., 1998), while others utilize self-consistent radiative transfer codes to predict observable properties (e.g., Young & Evans, 2005; Whitney et al., 2003). Ideally, a comparison between models and observed source properties will differentiate between the input initial conditions and assumed star formation models, as well as provide estimates of the accretion rate, age, and final mass for individual sources.

Figure 1.5 shows the results of simple evolutionary models from Myers et al. (1998), plotted as tracks on a bolometric luminosity versus bolometric temperature ($L_{bol} - T_{bol}$) diagram. The $L_{bol} - T_{bol}$ diagram for protostellar sources is analogous to the Hertzsprung-Russell (H-R) diagram (Hertzsprung, 1905; Russell, 1914) for more evolved objects. Protostellar cores do not have a well-defined photosphere, and

thus do not have a well-defined effective temperature. Instead, the temperature is quantified by T_{bol}, defined as the temperature of a blackbody with the same mean frequency $\langle\nu\rangle$ as the observed SED:

$$T_{bol} = \frac{\zeta(4)}{4\zeta(5)}\frac{h\langle\nu\rangle}{k} = 1.25 \times 10^{-11}\langle\nu\rangle \ \text{ K Hz}^{-1} \tag{1.9}$$

(Myers & Ladd, 1993). The mean frequency is the luminosity weighted mean,

$$\langle\nu\rangle = \frac{\int \nu S_\nu d\nu}{\int S_\nu d\nu}, \tag{1.10}$$

and $\zeta(n)$ is the Riemann zeta function.

Myers et al. (1998) develop analytic expressions for T_{bol} and L_{bol} as a function of time, assuming an accretion rate that is initially the Shu value, $dM/dt = c_s^3/G$, and then falls off exponentially with time. The emergent bolometric luminosity is the sum of the infall (accretion) and stellar contraction luminosities. They also assume that a significant fraction of the original core mass is dissipated during the star formation process ($M_{core}/M_* = 6$). This simple model was a good match to the properties of Class 0 and Class I sources known at the time, suggesting that accretion rates decrease with time after protostar formation. It must be reevaluated based on more complete samples and more sensitive data, however. More detailed models using accretion rates that are constant (Young & Evans, 2005), or derived from turbulent simulations (Froebrich et al., 2006), can also be tested against observations.

Mass accretion rates are directly linked to the length of time sources spend in any given evolutionary stage. The relative number of sources in sequential stages of evolution can be used as a simple measure of the relative lifetimes of those stages: $t_1/t_2 = N_1/N_2$. This kind of analysis relies on a number of assumptions, including that (1) star formation is steady in time, i.e. we are not observing sources at a special time in their evolution, (2) we have correctly categorized sources into a true evolutionary sequence, and (3) there are no significant variations of the lifetime with source mass. Observations of protostars in ρ Ophiuchi originally led to an extremely short estimate

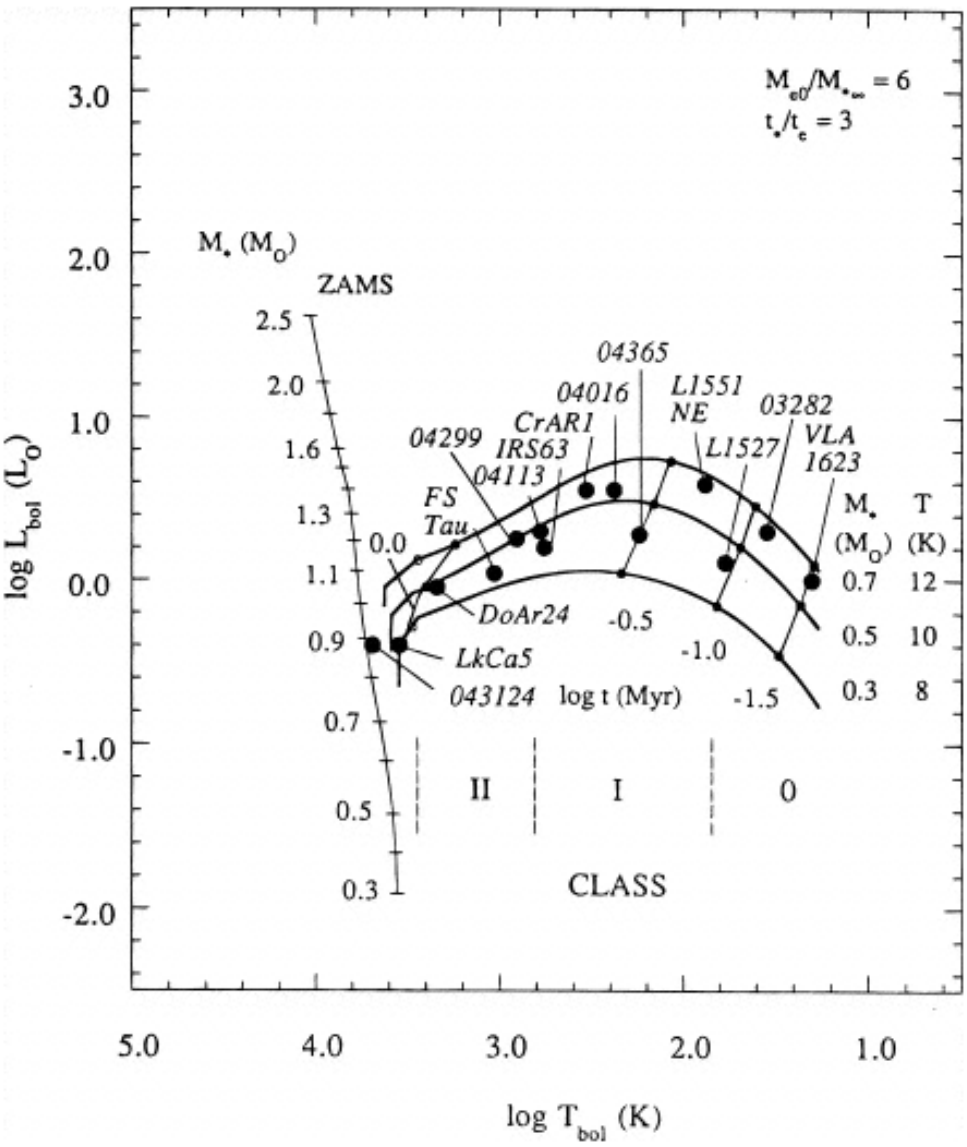

Figure 1.5 Simple models of the evolution of protostars from Myers et al. (1998), plotted on the bolometric luminosity-temperature diagram, and compared to data for young protostars available at the time. Myers et al. (1998) assume an exponentially decreasing accretion rate and derive analytic expressions for T_{bol} and L_{bol} as a function of time.

for the Class 0 phase, $t_{Class0} \sim 10^4$ yr, based on the relative number of Class 0 and Class I objects (André & Montmerle, 1994). Such a short Class 0 lifetime would require very high accretion rates immediately after protostellar formation. More recent studies of a sample of Lynds dark clouds (Visser et al., 2002) and protostars in Perseus (Hatchell et al., 2007) have concluded that the Class 0 lifetime is similar

to the Class I lifetime, approximately $2 - 4 \times 10^5$ yr.

The Class 0 lifetime can be used as a further test of protostellar evolutionary models, which predict varying lengths of time spent in the Class 0 phase. In the exponentially declining accretion rate models of Myers et al. (1998), a source with final stellar mass 0.3 $M_\odot$ reaches the end of the Class 0 phase (when $M_* = M_{env}$) at $t \sim 10^5$ yr. Young & Evans (2005) assume a constant Shu accretion rate, finding that $M_* = M_{env}$ at a much earlier time, $t \sim 3.5 \times 10^4$ yr. Froebrich et al. (2006) compare accretion rates predicted by numerical simulations of gravo-turbulent fragmentation models (Schmeja & Klessen, 2004) to a sample of observed protostars, finding a lifetime for Class 0 sources of $2 - 6 \times 10^4$ yr.

A complete census of young protostars is important for comparing to evolutionary models, and for calculating a statistically significant lifetime for the Class 0 phase. In contrast to less embedded sources, the highly obscuring envelopes of Class 0 sources make them invisible at short wavelengths, so sensitive mid- to far-infrared measurements are necessary to obtain a more complete picture of how protostars evolve through this early stage. Larger samples will provide more robust statistics, and help to differentiate the sometimes degenerate effects of environment, viewing geometry, and age.

1.1.6 Effects of Environment

Cloud environmental factors such as turbulence and average cloud density may have strong effects on the outcome of star formation. Nearly all of the observational measures discussed above may vary with large-scale cloud conditions, including the CMD, initial conditions of cores, protostellar accretion rates, and the efficiency of star formation. For example, starless cores in regions of clustered star formation are observed to have smaller radii and higher column density, by as much as an order of magnitude, than isolated cores. Even the dominant physical processes controlling core formation and evolution (e.g., quasi-static versus dynamic) may depend on environment (Ward-Thompson et al., 2007). Vázquez-Semadeni et al. (2005) suggest that the strength of

magnetic fields in turbulent clouds has a significant impact on the efficiency of star formation.

Differences with environment are important to quantify if we are to understand the implications of observations. In addition, it is important to know which observed properties do *not* seem to change with environment; e.g., if the IMF is truly universal but the CMD varies from cloud to cloud, any successful theory of star formation would be required to explain the discrepancy. Ideally, theories and simulations of star formation can make predictions based on varying environmental factors, enabling observations in different environments to place strong constraints on star formation models.

Several authors have been able to reproduce the slope of the IMF directly from turbulent fragmentation into cores (e.g., Padoan & Nordlund, 2002; Li et al., 2004), but special assumptions are often required. Ballesteros-Paredes et al. (2006) test the dependence on Mach number of the CMD resulting from smoothed particle hydrodynamics (SPH) simulations of turbulent fragmentation, finding that the emergent mass spectrum of dense cores depends strongly on the turbulent Mach number in the cloud (figure 1.6). The Mach number is a measure of the strength of turbulence: $\mathcal{M} = \sigma_v / c_s$, where σ_v is the rms velocity dispersion, $c_s = \sqrt{kT/\mu m_H}$ is the isothermal sound speed, and μ is the mean molecular weight per particle.

As demonstrated in figure 1.6, Ballesteros-Paredes et al. (2006) find that models with stronger turbulence (i.e. higher Mach numbers) result in a larger number of low mass cores and relatively few high mass cores (solid curve). Strong turbulence creates more sub-structure on smaller scales, thus favoring many cores of low mass. Conversely, weaker turbulence (lower Mach numbers) results in cores with higher masses in general, and significantly fewer low mass cores (dotted curve). Furthermore, the slope of the CMD for $M \gtrsim 0.3$ $M_\odot$ is noticeably flatter for the low Mach number models. These important differences make it possible to test predictions of simulations such as this one by measuring the core mass distribution in clouds with varying turbulent properties.

For the most part, previous samples of prestellar cores and very young protostars

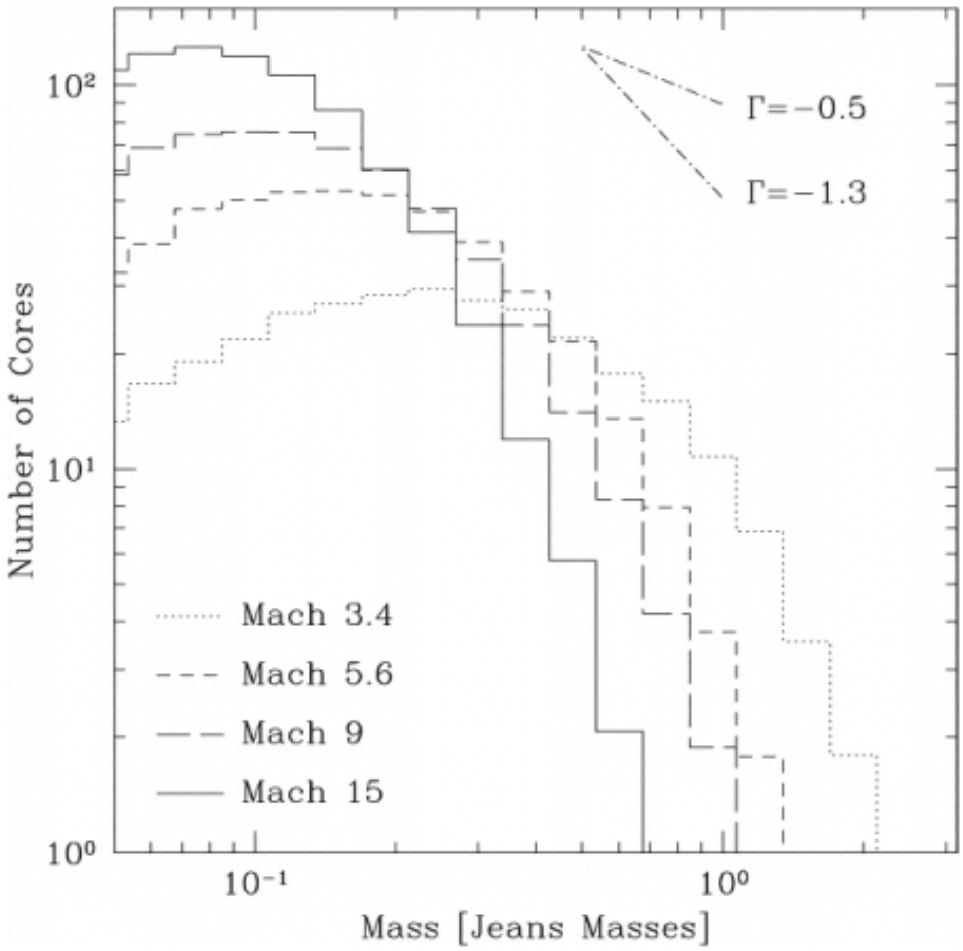

Figure 1.6 Core mass distributions resulting from the SPH turbulent fragmentation simulations of Ballesteros-Paredes et al. (2006), for a range of turbulent Mach numbers. Larger Mach numbers result in a higher fraction of low mass cores, and a steeper slope at the high mass end of the CMD.

have not been large enough to disentangle the effects of environment from systematic uncertainties and small number statistics. Many studies have combined data from different instruments or resulting from different reduction and analysis techniques, complicating the picture further. Large, unbiased, complete samples in a range of environments are necessary to test the effect of environment on the core mass distribution, the initial conditions and spatial distributions of cores, the star formation efficiency, and protostellar evolution.

1.2 Observations

In order to make significant progress on the problems described above, a complete census of starless cores and young protostars in molecular clouds is required. Thus large-scale observations of entire molecular clouds are necessary, particularly at far-infrared to millimeter wavelengths, where the emission from starless cores and deeply embedded protostars peaks. Sensitive mid-infrared data are also essential for the reliable identification of prestellar cores and characterization of young protostars. In addition, surveys of many different regions and in clouds with diverse properties are needed to address the possible environmental dependencies of the star formation process.

1.2.1 Millimeter Surveys

Large-scale millimeter-wavelength continuum surveys are essential for addressing the outstanding questions outlined in §1.1.2. Millimeter emission from molecular clouds traces the total mass of prestellar cores and protostellar envelopes, and is one of the best ways to detect prestellar cores, which are only visible at far-infrared to millimeter wavelengths. Furthermore, millimeter surveys provide a large-scale picture of the on-going star formation in molecular clouds by detecting the current, and even future, populations of star-forming cores.

Historically, most studies at submillimeter and millimeter wavelengths have focused on individual objects or small regions of less than 1 deg^2, due to instrumental limitations. Recently, however, the development of large-format bolometer arrays on 10 m class telescopes has made it possible to complete large-scale maps of nearby molecular clouds, covering many square degrees on the sky. Examples of currently operating bolometer arrays, and their characteristics, are given in table 1.1.

In the last few years, wide-field mapping of several nearby molecular clouds has been completed. Approximately 0.2 deg^2 of the Ophiuchus molecular cloud was mapped by Johnstone et al. (2000) at 850μm with SCUBA, while a larger 4 deg^2 map is referred to by Johnstone et al. (2004) and available from the COMPLETE

Table 1.1. Millimeter and submillimeter bolometer arrays

Telescope	Instrument	Wavelength(s)	Pixels	Field of view	Resolution	Reference
CSO	Bolocam	1.1, 1.4, 2.1 mm	144	$7\farcm5$[a]	$30''$[a]	(1)
CSO	SHARC II	350, 450, 850 μm	384	$2\farcm6 \times 1'$	$9''$	(2)
JCMT	SCUBA	450, 850 μm	37[b]	$2\farcm3$[b]	$14''$[b]	(3)
IRAM 30 m	MAMBO2	1.2 mm	117	$4'$	$11''$	(4)
SEST	SIMBA	1.2 mm	37	$5'$	$24''$	(5)

Note. — References: (1) Glenn et al. 1998; (2) Dowell et al. 2003; (3) Holland et al. 1999; (4) Kreysa et al. 1998; (5) Nyman et al. 2001. CSO: Caltech Submillimeter Observatory, JCMT: James Clerk Maxwell Telescope, SEST: Swedish-ESO Submillimetre Telescope.

[a]at $\lambda = 1.1$ mm

[b]at $\lambda = 850$ μm

website.[1] Most recently, Stanke et al. (2006) mapped 1.3 deg^2 in Ophiuchus at 1.2 mm with SIMBA. In the Perseus molecular cloud, Hatchell et al. (2005) mapped 3 deg^2 with SCUBA at 850 and 450μm. Combining SCUBA archive data with new observations of an additional 1.3 deg^2, Kirk et al. (2006) analyzed a total area of 3.5 deg^2. The Bolocam 1.1 mm surveys presented in this thesis cover significantly larger areas in Perseus (7.5 deg^2) and Ophiuchus (10.8 deg^2), and include a 1.5 deg^2 map of the Serpens molecular cloud.

1.2.1.1 Prestellar Cores

As is evident from the SED in figure 1.1, prestellar cores are only visible at wavelengths longer than about 50μm, and their SEDs peak at $200-400\mu$m. Consequently, submillimeter ($\lambda \sim 350-850\mu$m) and millimeter ($\lambda \sim 1-3$ mm) continuum observations are ideal for studying these cold objects. In contrast to FIR observations, which must be completed above the earth's atmosphere, (sub)mm observations can utilize large ground-based telescopes. Continuum surveys for prestellar cores also have advantages over spectral line and dust extinction studies. Even spectral line surveys

[1]http://cfa-www.harvard.edu/COMPLETE

using molecules with relatively high critical densities (e.g., NH_3, which is sensitive to $n_{H_2} \gtrsim 3 \times 10^3$ cm^{-3}), are generally sensitive to lower density material than millimeter observations, and can be subject to chemistry effects such as depletion, freeze-out, and evaporation (e.g., Lee, Bergin, & Evans, 2004). Dust extinction maps are sensitive to all material along the line of sight, not just that in dense cores, and are more likely than millimeter surveys to detect diffuse structures that will never form stars.

Observationally, it is difficult to separate true prestellar cores, which are gravitationally bound and will eventually collapse to form stars, from stable or unbound cores that will eventually disperse back into the general cloud medium. Throughout this thesis I follow Di Francesco et al. (2007) in defining "starless" cores as low mass dense cores without a compact internal luminosity source, "prestellar" cores, at least conceptually, as starless cores that are gravitationally bound, and "protostellar" cores as dense cores that already harbor a compact internal source. A practical method of distinguishing prestellar cores is required as well; our operational definition of a prestellar core is a starless core that is detected at submillimeter or millimeter wavelengths. Such sources have mean densities $\gtrsim 2 - 3 \times 10^4$ cm^{-3} (see Ward-Thompson et al. 1994 and chapter 5), and are more likely to show evidence for infall motions than lower density starless cores (Gregersen & Evans, 2000).

1.2.1.2 Masses

Dust grains in cold ($5 - 30$ K), dense ($n \gtrsim 10^4$ cm^{-3}) prestellar and protostellar cores produce thermal emission at far-infrared (FIR) to millimeter wavelengths. The relationship between the observed flux from an individual source of millimeter continuum emission and the mass of dust in that source can be easily derived. Radiative transfer gives us the flux density from a spherical source of dust emission at a frequency ν:

$$F_\nu = \int I_\nu \cos\theta d\Omega, \tag{1.11}$$

where

$$I_\nu = \int \rho \kappa_\nu S_\nu ds \tag{1.12}$$

is the specific intensity, $S_\nu = B_\nu(T_D)$ is the source function, ρ is the mass density of dust, T_D is the dust temperature, and κ_ν is the dust opacity at frequency ν. Integrations are over source solid angle in equation (1.11), and line-of-sight distance in equation (1.12).

Assuming that the emission is optically thin at the observed frequency. and that κ_ν and ρ do not vary with position, the integral in equation (1.12) simplifies to:

$$I_\nu = \rho\kappa_\nu B_\nu(T_D)\int_{-R}^{R} ds = 2R\rho\kappa_\nu B_\nu(T_D), \tag{1.13}$$

where R is the radial extent of the source. Combining equations (1.11) and (1.13) produces

$$F_\nu = \rho\kappa_\nu B_\nu(T_D)\int_0^{2\pi} d\phi \int_0^{\theta_c} 2Rsin^2\theta\cos\theta d\theta = \rho\kappa_\nu B_\nu(T_D)2\pi d\frac{\sin^3\theta_c}{3}, \tag{1.14}$$

where $\sin\theta_c = R/d$ and d is the distance to the source. Finally,

$$F_\nu = \frac{4\pi}{3}\frac{R^3}{d^2}\rho\kappa_\nu B_\nu(T_D) = M_D\frac{\kappa_\nu B_\nu(T_D)}{d^2}, \tag{1.15}$$

where we have assumed a spherical source and substituted the total mass of dust: $M_D = \frac{4}{3}\pi R^3\rho$.

Thus for optically thin emission the observed flux density of a core is proportional to the total mass of dust, and equation (1.15) can be inverted to give us the mass:

$$M_D = \frac{d^2 S_\nu}{B_\nu(T_D)\kappa_\nu}. \tag{1.16}$$

Although the millimeter emission arises only from the dust and not the gas that provides the majority of mass in a core, we can infer the total mass of gas *and* dust by assuming a gas to dust mass ratio of 100, which is generally included in the value of κ_ν. As long as the bulk of a given core remains optically thin at millimeter wavelengths, this equation provides a straightforward method for measuring the total mass in starless cores and protostellar envelopes, assuming κ_ν is known.

Directly measuring the (sub)mm emissivity, or equivalently the opacity κ_ν, of dust in molecular clouds and dense cores is extremely difficult, as it requires independent knowledge of the amount of dust present (e.g., Alton et al., 2000). Although the wavelength dependence of dust extinction in the interstellar medium is well known, and has been successfully characterized by models of grain composition and size distributions together with synthesized dialectric functions of grain components (Mathis, Rumpl, & Nordsieck, 1977; Draine & Lee, 1984), dust grains in dense cores differ from those in the general interstellar medium due to grain coagulation and the formation of molecular ice mantles. The optical properties of such particles are a sensitive function of the assumed structure and chemical composition of the grains; detailed modeling of the accretion and coagulation of dust grains are necessary to calculate the opacity as a function of wavelength (Ossenkopf & Henning, 1994).

Resulting opacities still vary by at least a factor of two ($\kappa_{1mm} \sim 0.008 - 0.017$ cm^2 g^{-1}; Ossenkopf & Henning 1994), depending on gas density and coagulation time, and must be constrained using high-resolution observations of individual cores, together with radiative transfer modeling (e.g., Shirley, Evans, & Rawlings, 2002; Young et al., 2003) or comparison to extinction from deep near-infrared maps (e.g., Bianchi et al., 2003). Here I adopt $\kappa_{1mm} = 0.0114$ cm^2 g^{-1}, with the caveat that all masses retain an uncertainty of at least a factor of two. This value is interpolated from Ossenkopf & Henning (1994) table 1 column 5, for dust grains with thin ice mantles, coagulated for 10^5 years at a gas density of 10^6 cm^{-3}.

1.2.2 Infrared Surveys

When millimeter surveys are combined with *Spitzer* infrared data they provide an even more powerful probe of star formation. Detecting and characterizing the compact, accreting objects embedded within protostellar cores requires information at mid- to far-infrared wavelengths to complete the story. Sensitive infrared data, especially from $\lambda \sim 10\mu$m to a few $\times 100\mu$m, are necessary for calculating source spectral energy distributions, as well as properties such as L_{bol} and T_{bol}, which are essential

for comparisons to evolutionary models. Furthermore, infrared data are required to identify starless cores, and to make the accurate classifications of protostellar sources needed to estimate the lifetimes of evolutionary stages.

The Bolocam 1.1 mm maps of Serpens, Perseus, and Ophiuchus presented in this thesis are coordinated to cover the same regions as *Spitzer* Space Telescope Infrared Array Camera (IRAC) and Multiband Imaging Photometer for Spitzer (MIPS) maps from the "Cores to Disks" *Spitzer* Legacy program. IRAC consists of four arrays simultaneously viewing the sky at $\lambda = 3.6$, 4.5, 5.8, and 8.0 μm, while MIPS images at $\lambda = 24$, 70, and 160μm simultaneously. Thus *Spitzer* maps provide complete wavelength coverage from 3.6 to 1100μm when combined with the Bolocam data.

1.2.2.1 "Cores to Disks" Legacy Program

As part of the *Spitzer* Legacy program "From Molecular Cores to Planet-forming Disks" ("Cores to Disks" or c2d; Evans et al. 2003), the five nearest large molecular clouds, including Perseus, Serpens, and Ophiuchus, were mapped with IRAC and MIPS on the *Spitzer* Space Telescope. The c2d IRAC and MIPS maps cover 3.9 and 10.6 deg^2, respectively, in Perseus, 0.9 and 1.5 deg^2 in Serpens, and 6.6 and 13.7 deg^2 in Ophiuchus. *Spitzer* observations were designed to cover down to $A_V \sim 2$ mag in the Perseus cloud based on the ^{13}CO map of Padoan et al. (1999), and $A_V \sim 3$ mag in Ophiuchus and $A_V \sim 6$ mag in Serpens based on the visual extinction maps of Cambrésy (1999). Goals of the c2d project include determining how the youngest stars and protostars are distributed in position and mass, and using unbiased determinations of cloud populations to measure statistical lifetimes for various evolutionary stages (Evans et al., 2003).

All data from the c2d project, including post-pipeline improved images and catalogs containing IRAC and MIPS (24, 70μm) fluxes of all detected sources in each cloud, are publicly available (Evans et al., 2007). Near-infrared data are also included in the c2d catalogs for sources that appear in the Two Micron All Sky Survey (2MASS) catalogs. Photometry at 160μm has been calculated by the c2d team for point-like sources in the MIPS 160μm maps, but is not included in the public cat-

alogs. Data reduction, mapping, and source extraction are described in detail in a series of "basic data papers" (e.g., Jørgensen et al., 2006; Harvey et al., 2006; Rebull et al., 2007), in which cloud maps are also presented. Harvey et al. (2007) discuss the method for identifying young stellar object (YSO) candidates, which cover the range from infrared-excess stars to deeply embedded protostars. A careful accounting for extragalactic contamination is also included in Harvey et al. (2007).

1.3 Thesis Goals and Outline

As already indicated, there are a number of outstanding questions that remain regarding the formation of low mass stars in molecular clouds. The nature of the dominant physical processes controlling the formation and support of prestellar cores, and their subsequent collapse into protostars, is still a matter of debate. Initial conditions of the prestellar core populations of molecular clouds are important probes of the star formation process, including cloud support, core formation, and core collapse physics. In particular, the prestellar core mass distribution and the lifetime of prestellar cores provide important tests of star formation theories. The evolution of protostars from initial core collapse through the main accretion phase, including mass accretion rates and timescales, have remained difficult to characterize due to the highly embedded nature of such sources. A combination of millimeter and far-infrared observations are necessary to understand these deeply embedded sources. Finally, relatively little is understood about how the star formation process depends on environmental factors such as average cloud density or the strength of large-scale turbulence. Addressing this question requires large-scale surveys in many different star-forming environments.

The goal of this thesis is to address each of these important issues. To that end, I utilize large-scale, $\lambda = 1.1$ mm dust continuum surveys in combination with deep *Spitzer* IRAC and MIPS maps, to build a complete sample of the youngest star-forming objects in three nearby molecular clouds. Chapters 2, 3, and 4 present the basic results of Bolocam 1.1 mm continuum surveys of the Perseus, Ophiuchus, and Serpens molecular clouds, respectively. Also in chapter 2, I introduce the 1.1 mm

survey techniques and basic data reduction procedures, and describe an iterative mapping routine that I developed for the Bolocam reduction pipeline, which is essential for analysis of the molecular cloud data. Results from the Perseus survey include source identifications and fundamental source properties such as fluxes, sizes, shapes, masses. The relationship between dense cores and other column density tracers such as visual extinction and ^{13}CO molecular line mapping is also discussed, as is the spatial clustering properties of cores. This chapter has already been published (Enoch et al., 2006).

Results from the Ophiuchus and Serpens surveys are presented in a similar way in chapters 3 and 4. They are accompanied by relatively little analysis, and are intended to provide the basic source properties, as well as background information about the clouds and observations. The Ophiuchus survey was led by graduate student Kaisa Young at the University of Texas, Austin (Young et al., 2006). Reduction and analysis of that cloud followed the pipeline I established, however. I also contributed significantly to the interpretation and writing of the published paper.

In chapter 5, I compare the properties of the millimeter core populations in the three molecular clouds, to better understand the environmental dependencies of low mass star formation. The physical implications of core sizes and shapes are discussed, and the relative shapes of the cloud core mass distributions are compared to simulations. I look at the cloud-to-cloud similarities and differences in spatial clustering properties, core formation efficiency, and in the relationship between dense cores and cloud column density. This analysis, together with the Serpens results, are included in a paper accepted to ApJ, and currently in press.

Bolocam maps of each cloud are combined with *Spitzer* data from the c2d Legacy project in chapter 6, enabling a separation of starless and protostellar cores. I measure the initial conditions of the starless core populations in each cloud, including masses, sizes, shapes, and mean densities, and compare the starless and protostellar populations to infer how the formation of a central protostar alters core properties. The prestellar core mass distribution is constructed from the combined starless core samples, and compared to the initial mass function of stars. Complete SEDs of cold

protostellar candidates, from $\lambda = 1.25 - 1100\mu$m, are used to calculate source properties such as bolometric luminosities, bolometric temperatures, and envelope masses, and to classify sources into an evolutionary sequence. I compare protostellar sources in each cloud to evolutionary models in order to draw conclusions about mass accretion rates, and place constraints on models. Finally, the relative number of sources in different evolutionary stages are used to estimate lifetimes for the prestellar and Class 0 phases.

A brief summary of this thesis, and discussion of future projects that can build upon this work to more fully understand the formation of low mass stars in molecular clouds, is presented in chapter 7.

Bibliography

Adams, F. C., Lada, C. J., & Shu, F. H. 1987, ApJ, 312, 788

Adams, F. C., & Shu, F. H. 1986, ApJ, 308, 836

Alton, P. B., Xilouris, E. M, Bianci, S., Davies, J., Kylafis, N. 2000, A&A, 356, 795

Alves, J., Lombardi, M., & Lada, C. J. 2007, A&A, 462L, 17

André, P. 1994, in *The Cold Universe*, Editors T. Montmerle, C. J. Lada, I. F. Mirabel, & J. Tran Thanh Van, p. 179

André, P. 1996, in *Memorie della Societa Astronomia Italiana*, vol. 67, p. 901

André, P. & Montmerle, T. 1994, ApJ, 420, 837

André, P., Ward-Thompson, D., & Barsony, M. 1993, ApJ, 406, 122

Bachiller, R. 1996, ARA&A, 34, 111

Ballesteros-Paredes, J., Gazol, A., Kim, J., Klessen, R. S., Jappsen, A-K., & Tejero, E., 2006, ApJ, 637, 384

Ballesteros-Paredes, J., Klessen, R. S., & Vázquez-Semadeni, E. 2003, ApJ, 592, 188

Bianchi, S., Gonalves, J., Albrecht, M., Caselli, P., Chini, R., Galli, D., Walmsley, M. 2003, A&A, 399, L43

Bonnell, I. A., Bate, M. R., Clarke, C. J., & Pringle, J. E. 2001, 323, 785

Bonnor, W. B. 1956, MNRAS, 116, 351

Bourke, T. L., Hyland, A. R., Robinson, G., James, S. D., & Wright, C. M. 1995, MNRAS, 276, 1067

Cambrésy, L. 1999, A&A, 345, 965

Chabrier, G. 2005 in The Stellar Initial Mass Function Fifty Years Later, editors E. Corbelli, F. Palla, and H. Zinnecker, p. 41

Di Francesco, J., Evans, N. J., II, Caselli, P., Myers, P. C., Shirley, Y., Aikawa, Y., & Tafalla, M. 2007, in Protostars and Planets V, editors B. Reipurth, D. Jewitt, and K. Keil, p. 17

Dowell, C. D., Allen, C. A., Babu, R. S., Freund, M. M., Gardner, M., Groseth, J., Jhabvala, M. D., et al. 2003, SPIE, 4855, 73

Draine, B. T., & Lee, H. M. 1984, ApJ, 285, 89

Ebert, R. 1955, Zeitschrift Astrophysics, 37, 217

Enoch, M. L., Young, K. E., Glenn, J., Evans, N. J., II, Golwala, S., Sargent, A. I., Harvey, P., et al. 2006, ApJ, 638, 293

Evans, N. J., II 1999, ARA&A, 37, 311

Evans, N. J., II, Allen, L. E., Blake, G. A., Boogert, A. C. A., Bourke, T., Harvey, P. M., Kessler, J. E., et al. 2003, PASP, 115, 965

Evans, N. J., II, et al. 2007, Final Delivery of Data from the c2d Legacy Project: IRAC and MIPS

Froebrich, D., Schmeja, S., Smith, M. D., & Klessen, R. S. 2006, MNRAS, 368, 435

Glenn, J., Bock, J. J., Chattopadhyay, G., Edgington, S. F., Lange, A. E., Zmuidzinas, J., Mauskopf, P. D., Rownd, B., Yuen, L., & Ade, P. A. 1998, SPIE, 3357,326

Gregersen, E. M. & Evans, N. J., II 2000, ApJ, 538, 260

Harvey, P. M., Chapman, N., Lai, S.-P.. Evans, N. J., II, Allen, L. E., Jørgensen, J. K., Mundy, L. G., et al. 2006, ApJ, 644, 307

Harvey, P. M., Merin, B., Huard, T. L., Rebull, L. M., Chapman, N. Evans, N. J., II, & Myers, P. C. 2007, ApJ, in press (preprint: arXiv:0704.0009 [astro-ph])

Hatchell, J., Fuller, G. A., Richer, J. S., Harries, T. J., & Ladd, E. F. 2007, A&A, accepted (preprint:astro-ph/0612601)

Hatchell, J., Richer, J. S., Fuller, G. A., Qualtrough, C. J., Ladd, E. F., & Chandler, C. J. 2005, A&A, 440, 151

Henriksen, R., Andre, P., & Bontemps, S. 1997, A&A, 323, 549

Hertzsprung, E. 1905, Sur Strahlung der Sterne (Z. Wiss Photog., 3)

Holland, W. S., Robson, E. I., Gear, W. K., Cunningham, C. R., Lightfoot, J. F., Jenness, T., Ivison, R. J., et al. 1999, MNRAS, 303, 659

Hoyle, F. 1953, ApJ, 118, 513

Jayawardhana, R., Hartmann, L., Calvet, N. 2001, ApJ, 548, 310

Jeans, J. H. 1928, Astronomy and Cosmogony, p. 340

Jessop, N. E., & Ward-Thompson, D. 2000, MNRAS, 311, 63

Johnstone, D., DiFrancesco, J., & Kirk, H. 2004, ApJ, 45, 611L

Johnstone, D., Wilson, C. D., Moriarty-Schieven, G., Joncas, G., Smith, G., Gregersen, E., & Fich, M. 2000, ApJ, 545, 327

Jørgensen, J. K., Johnstone, D., Kirk, H., & Myers, P. C. 2007, ApJ, 656, 293

Jørgensen, J. K., Harvey, P. M., Evans, N. J., II, Huard, T. L., Allen, L. E., Porras, A., Blake, G. A., et al. 2006, ApJ, 645, 1246

Kirk, H., Johnstone, D., & DiFrancesco, J. 2006, ApJ, 646, 1009

Kreysa, E., Gemuend, H.-P., Gromke, J., Haslam, C. G., Reichertz, L., Haller, E. E., Beeman, J. W., Hansen, V., Sievers, A., & Zylka, R. 1998 SPIE, 3357, 319

Kroupa, P. 2002, Science, 295, 82

Lada, C. J. 1987, In Star Forming Regions, IAU Symp. 115, editors M. Peimbert, J. Jugaku, p. 1

Lada, C. J., & Lada, E. A. 2003, ARA&A, 41, 57

Lada, C. J. & Wilking, B. A. 1984, ApJ287,610

Lee, J.-E., Bergin, E. A., & Evans, N. J., II 2004, ApJ, 617, 360

Lee, W. C., & Myers, P. C. 1999, ApJS, 123, 233

Li, P. S., Norman, M. L., Mac Low, M., & Heitsch, F. 2004, ApJ, 605, 800

Luhman, K. L., Stauffer, J. R., Muench, A. A., Reike, G. H., Lada, E. A., Bouvier, J., & Lada, C. J. 2003, ApJ, 593, 1115

Mac Low, M.-M., & Klessen, R. S. 2004, RevPhys, 76, 125

Mathis, J. S., Rumpl, W., & Nordsieck, K. H. 1977, ApJ, 217, 425

McKee, C. F. 1989, ApJ, 345, 782

McKee, C. F., & Zweibel, E. G. 1992, ApJ, 399, 551

McLaughlin, D. E. & Pudritz, R. E. 1997, ApJ, 476, 750

Meyer, M. R., Adams, F .C., Hillenbrand, L. A., Carpenter, J. M., & Larson, R. B. 2000, in Protostars and Planets IV, editors V. Mannings, A. P. Boss, & S. S. Russell, p. 121

Motte, F., André, P., & Neri, R. 1998, A&A, 336, 150

Muench, A. A., Lada, E. A., Lada, C. J., & Alves, J. 2002, ApJ, 573, 366

Myers, P. C. 1998, ApJ, 496, L109

Myers, P. C., Adams, F. C., Chen, H., & Schaff, E. 1998, ApJ, 492, 703

Myers, P. C. & Benson, P. J. 1983, ApJ, 266, 309

Myers, P. C. & Ladd, E. F. 1993, ApJ, 413, L47

Nakano, T. 1998, ApJ, 494, 587

Nyman, L.-Å., Lerner, M., Nielbock, M., et al. 2001, The Messenger, 106, 40

Onishi, T., Kawamura, A., Tachihara, K., & Fukui, Y. 2002, ApJ, 575, 950

Ossenkopf, V., & Henning, Th. 1994, A&A, 291, 943

Padoan, P., Bally, J., Billawala, Y., Juvela, M., & Nordlund, Å. 1999, ApJ, 525, 318

Padoan, P., & Nordlund, Å. 2002, ApJ, 576, 870

Palla, F., & Stahler, S. W. 2002, ApJ, 581, 1194

Rebull, L. M., Stapelfeldt, K. R., Evans, N. J., II, Joergensen, J. K., Harvey, P. M., Brooke, T. Y., Bourke, T. L., et al. 2007, ApJ, in press (preprint:stro-ph/0701711)

Reid, I. N., Gizis, J. E., & Hawley, S. L. 2002, AJ, 124, 2721

Russell, H. N. 1914, Pop. Astron., 22, 275, 321

Salpeter, E. E. 1955, ApJ, 121, 161

Scalo, J. M. 1986, Fundam. Cosmic Phys., 11, 1

Scalo, J. M. 2005 in The Stellar Initial Mass Function Fifty Years Later, editors E. Corbelli, F. Palla, and H. Zinnecker, p. 23

Schmeja, S. & Klessen, R. S. 2004 A&A, 419, 405

Schröder, K.-P.,& Pagel, B. E. J. 2003, MNRAS, 343, 1231

Shirley, Y. L., Evans, N. J., II, & Rawlings, J. M. C. 2002, ApJ, 575, 337

Shu, F. H. 1977, ApJ, 214, 488

Shu, F. H., Adams, F. C., & Lizano, S. 1987, ARA&A, 25, 23

Shu, F. H., Najita, J., Galli, D., Ostriker, E., & Lizano, S. 1993 In: Protostars and planets III p. 3

Spitzer, L. Jr. 1968, Diffuse Matter in Space

Spitzer, L. Jr. 1978, Physical Processes in the Interstellar Medium, p. 282

Stanke, T., Smith, M. D., Gredel, R., & Khanzadyan, T. 2006, A&A447, 609

Testi, L., & Sargent, A. I. 1998, ApJ, 508, L91

Vázquez-Semadeni, E., Kim, J., Shadmehri, M., & Ballesteros-Paredes, J. 2005, ApJ, 618, 344

Visser, A. E., Richer, J. S., & Chandler, C. J. 2002, AJ, 124, 2756

Ward-Thompson, D., André, P., Crutcher, R., Johnstone, D., Onishi, T., & Wilson, C. 2007, in Protostars and Planets V, editors B. Reipurth, D. Jewitt, and K. Keil, p. 33

Ward-Thompson, D., Scott, P. F., Hills, R. E., & Andre, P. 1994, MNRAS, 268, 276

White, R. J., Greene, T. P., Doppmann, G. W., Covey, K. R., Hillenbrand, L. A. 2007, in Protostars and Planets V, editors B. Reipurth, D. Jewitt, and K. Keil, p. 117

Whitney, B. A., Wood, K., Bjorkman, J. E., & Cohen, M. 2003, ApJ, 598, 1079

Wilking, B. A., 1989, PASP, 101, 229

Young, C. & Evans, N. J., II 2005, ApJ, 627, 293

Young, C. H., Shirley, Y. L., Evans, N. J., II, & Rawlings, J. M. C. 2003, ApJS, 145, 111

Young, K. E., Enoch, M. L., Evans, N. J., II, Glenn, J., Sargent, A., Huard, T. L., Aguirre, J., et al. 2006, ApJ, 644, 326

Zuckerman, B. & Palmer, P. 1974, ARA&A, 12, 279